Materials Today Energy 50 (2025) 101848

Contents lists available at ScienceDirect

Materials Today Energy

journal homepage: www.journals.elsevier.com/materials-today-energy/

Cost-effective and efficient preparation of $FePO_4$ electrodes from spent $LiFePO_4$ batteries for enhanced lithium extraction from salt lakes

Yawen Gao [a], Luxiang Ma [a,*], Shuaifei Zhao [b], Chunxi Hai [a], Tiandong Chen [a], Junyi Zhang [a], Yan Zhao [a], Yanxia Sun [a], Shengde Dong [a], Xin He [a], Qi Xu [a], Xiaowang Wu [c], Caixiong Quan [c], Hongli Su [b,**], Yuan Zhou [a,***]

[a] College of Materials and Chemistry & Chemical Engineering, Cheng Du University of Technology, Cheng Du, 610059, PR China
[b] Resource & Recycling, Department of Engineering Structures, Faculty of Civil Engineering and Geosciences, Delft University of Technology, Delft, 2628 CN, the Netherlands
[c] Qinghai Zhongxin Guoan Lithium Development Co., LTD, Qinghai Key Laboratory of Comprehensive Utilization of sulfate salt lake resources, Ge Er Mu, 816000, PR China

ARTICLE INFO

Keywords:
Lithium extraction
Electrochemical delithiation method
Spent lithium-ion battery
Cost-effective
Salt lake

ABSTRACT

Cost-effective and efficient lithium extraction technology is vital to foster the growth of lithium industry. This paper proposed a novel approach for the high value utilization of spent $LiFePO_4$ (S-$LiFePO_4$) in the field of lithium extraction from salt lakes was proposed using spent $LiFePO_4$ (S-$LiFePO_4$) as raw material. The anode, made from spent $LiFePO_4$, is prepared via a sintering process, while $FePO_4$, obtained through chemical oxidation, is used as the cathode. Compared with commercial $LiFePO_4$, this system not only reduces the cost but also greatly shortens the preparation time of $FePO_4$ (only about 10min is required). And the electrochemical extraction system had a favorable lithium extraction capacity (29.25 mg/g) from actual brine, reducing the Mg/Li ratio from 61.4 to 0.8. This study not only achieved the low-cost preparation of electrode materials and facilitated the large-scale implementation of this process, but also proposed a high-value comprehensive utilization strategy for lithium-ion batteries recycling.

1. Introduction

Lithium is a critical strategic resource extensively utilized across various sectors including energy, chemicals, and electronics [1]. The lithium-ion batteries (LIBs) expanded rapidly in the new energy automobile industry, leading to a substantial increase in demand for lithium resources. Global lithium resources are primarily found in ores, salt brines, and seawater, with approximately 70 % of lithium sourced from salt lake brines [2,3]. Compared with the high pollution of lithium extraction from ores and the low concentration of lithium resources in seawater, lithium extraction from saline lakes offers unique advantages, including low cost and environmental friendliness, and is expected to become the primary approach of lithium salt production [4,5]. China is a major lithium-producing country, with salt lake lithium resources account for 71.89 % of the total reserves [6]. However, most Chinese salt lakes are characterized by a high magnesium-to-lithium ratio. In addition, the quality of these salt lakes is gradually declining with the exploitation of high-quality salt lake resources. Therefore, there is an urgent need to develop low-cost and efficient methods for lithium extraction from these salt lakes.

Compared with adsorption, electrodialysis, nanofiltration, extraction, and other techniques, the electrochemical de-intercalation method offers the unique advantages of high selectivity for lithium ions and broad applicability to salt lake grades. This method has emerged as a prominent new technology for lithium extraction [7,8]. This method utilizes lithium-rich material as the anode and lithium-poor material as the cathode. By optimizing the applied potential, lithium ions are selectively removed from the salt lake brine, thereby facilitating the separation and extraction process of lithium ions. At present, the common electrode materials in this system include $LiMn_2O_4$, $LiFePO_4$, LNMO, etc. [9–11]. In contrast, $LiFePO_4$ is the preferred as electrode material for electrochemical delithiation due to its suitable working

* Corresponding author.
** Corresponding author.
*** Corresponding author.
E-mail addresses: maluxiang@cdut.edu.cn (L. Ma), suhong@deakin.edu.au (H. Su), zhouy@cdut.edu.cn (Y. Zhou).

https://doi.org/10.1016/j.mtener.2025.101848
Received 8 January 2025; Received in revised form 11 February 2025; Accepted 20 February 2025
Available online 28 February 2025

potential, structural stability, and high lithium-ion adsorption capacity [12,13]. For example, Yin et al. [14] prepared a porous $LiFePO_4$ electrode using PEG, which not only reduced electrode polarization and enhanced lithium diffusion within the electrode but also improved the selectivity and lithium extraction capacity of the system. In the $LiFePO_4$|supporting electrolyte anion exchange membrane|brine|$FePO_4$ system, The $FePO_4$ cathode used must have an olivine structure similar to that of $LiFePO_4$ to effectively separate and extract Li^+. The traditional $LiFePO_4$/$FePO_4$ electrode system employs commercial $LiFePO_4$ as the anode and produces $FePO_4$ with an olivine structure similar to $LiFePO_4$ as the cathode through electrochemical electrolysis [15]. However, this method is characterized by a complex process, lengthy electrode preparation times, low efficiency, and high costs, making it difficult to scale up. In recent years, Camille et al. [16] have prepared olivine structure $FePO_4$ with an olivine structure from sarcopside using a direct thermal oxidation method. Similarly, Xiong et al. [17] directly prepared $FePO_4$ with an olivine structure from commercial $LiFePO_4$ through chemical oxidation, which addressed key issues such as the complex electrode preparation process and long preparation times to some extent. However, both commercial $LiFePO_4$ and olivine-like $FePO_4$ are relatively expensive as electrode materials, highlighting the need for the development of low-cost and high-efficiency alternatives for industrial applications. As a by-product of the rapid development of the new energy industry, The market price of S-$LiFePO_4$ powder is about 41 % lower than that of commercial $LiFePO_4$ [18]. Moreover, studies have shown that most $LiFePO_4$ failures are due to loss of active lithium or electrolyte degradation [19,20], while the olivine-like crystal structure of $LiFePO_4$ remains. Thus, utilizing S-$LiFePO_4$ material for electrochemical delithiation to extract lithium can significantly reduce costs. Du et al. [21] used unmodified S-$LiFePO_4$ as the cathode and platinum (Pt) as the anode to investigate lithium extraction from salt lakes. However, this approach faces several challenges. Firstly, the high cost of precious metals makes the process expensive. Secondly, the specific capacity of lithium extraction achieved by electrochemical lithium extraction in their study is relatively low.

Therefore, a new concept of high value utilization of S-$LiFePO_4$ in the field of lithium extraction in salt lakes is proposed in this paper, which not only realizes the low-cost preparation of olivine-like $FePO_4$ electrode materials, but also promotes the large-scale promotion and production of this process. Moreover, it can realize the ecological, environmental protection and sustainable development route of lithium extraction from the salt lake, to the power battery, to the positive electrode of the waste lithium battery, and then to the lithium extraction from the salt lake. This paper proposed a new concept of high-value utilization of S-$LiFePO_4$ in the field of lithium extraction from salt lakes, that is, all electrode materials are from S-$LiFePO_4$. The process flow of the R-$LiFePO_4$/$FePO_4$ system is shown in Fig. 1, The high-efficiency adsorption of lithium ions in salt lake brine was achieved by using repaired $LiFePO_4$ (as an anode), and olivine $FePO_4$ (as a cathode) prepared by $Na_2S_2O_8$ (as an oxidant). The electrochemical extraction system had a favorable lithium extraction capacity (29.25 mg/g) for actual brine, with Mg/Li ratio decreasing from 61.4 to 0.8. Compared with the commercial R-$LiFePO_4$/$FePO_4$ system, the process not only reduces the cost, but also greatly improves the electrode preparation efficiency, which has certain reference significance for the low-cost and high-efficient preparation of electrode materials in the later electrochemical delithiation method.

2. Materials and methods

2.1. Reagents and materials

Sodium persulfate ($Na_2S_2O_8$), lithium chloride (LiCl), sodium chloride (NaCl), potassium chloride (KCl), calcium chloride ($CaCl_2$), and magnesium chloride hexahydrate ($MgCl_2{\cdot}6H_2O$) were purchased from Inokai Technology Co., Beijing, China. Polyvinylidene fluoride (PVDF) and Super P (C) were acquired from Kejing Material Technology Co., Hefei, China. N-methyl pyrrolidone (NMP) was purchased from Aladdin Biochemical Technology Co., Shanghai, China. deionized water. Spent lithium iron phosphate powder was artificially recycled by dismantling after discharging used $LiFePO_4$ batteries from the laboratory in a saturated NaCl solution. Deionized (DI) water with a resistivity of ~1.6×10^{-4} s/*m* was prepared by a Milli-Q ultrapure water purification system (Merck).

2.2. The preparation of $FePO_4$ electrodes

After preheating deionized water (500 mL) heated in a thermostatic water bath 40 °C, $Na_2S_2O_8$ (0.1 M) was added and stirred until completely dissolved. Then, spent $LiFePO_4$ powders (10 g) were added into the $Na_2S_2O_8$ solution to react for 10 min. After the reaction is completed, filter the product, wash it at least three times, and dry it at 80 °C for 8 h to obtain $FePO_4$ powder. Next $FePO_4$ powder, PVDF, and Super P were mixed evenly at a mass ratio of 8:1:1, and NMP was used as the solvent and stirred to obtain $FePO_4$ slurry, which was then coated, dried, and cut into pieces to obtain $FePO_4$ electrode.

2.3. Repair of S-$LiFePO_4$

The S-$LiFePO_4$ powder was placed in a tubular furnace under an Ar atmosphere. Using two-stage heating, the furnace temperature was first heated to 450 °C for 4 h, and then heated to 700 °C for 6 h, heating and cooling rates are 5 °min^{-1}, cooled to room temperature to obtain R-$LiFePO_4$ powder.

2.4. Preparation of R-$LiFePO_4$ electrode

The R-$LiFePO_4$ powder, PVDF, and Super P were added at a mass ratio of 8:1:1 for sufficient mixing. Then, the solvent NMP was added and stirred for 5 h to obtain the electrode slurry. After coating, drying, and cutting, the R-$LiFePO_4$ electrode was obtained. The S-$LiFePO_4$ electrode was prepared by the same method as above.

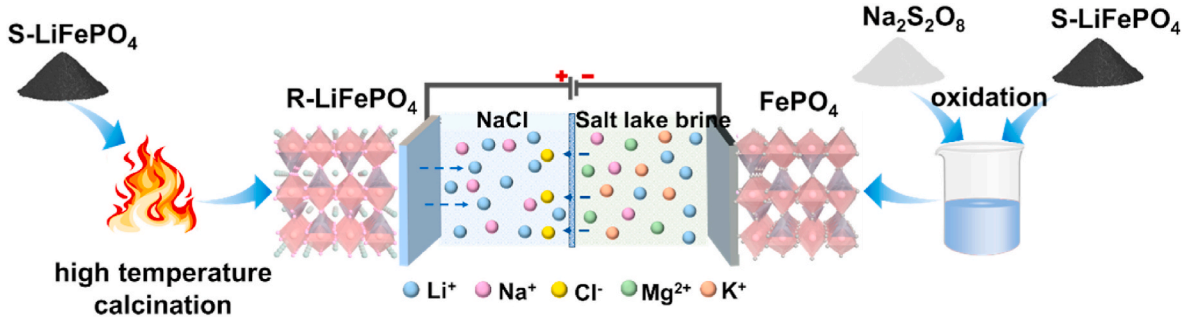

Fig. 1. Diagram of the preparation process of R-$LiFePO_4$/$FePO_4$ system.

2.5. Sample structure characterization

The crystal structure and lattice parameters of the three samples were analyzed using X-ray diffractometry (Rigaku Mini Flex 600, Japan) with a scanning range of 10°–80° and a scanning speed of 1°/min. The micromorphology was examined by scanning electron microscopy (FE-SEM, FEI Quantum 650, USA). The microstructure, element distribution, crystal phase, and lattice information of the electrode were characterized using field emission transmission electron microscopy (JEOL JEM 2100F). The types and valence states of elements on the surface of the three samples were determined by X-ray photoelectron spectroscopy (Shimadzu/Krayos AXIS Ultra DLD, Japan). The functional groups present in the samples were identified using infrared spectroscopy (Thermo Fisher Scientific Nicolet iS20, USA). The element content and composition of the materials were measured via inductively coupled plasma atomic emission spectrometry (ICP-AES Thermo Fisher, USA), while molecular vibration and carbon composition were analyzed using Raman spectroscopy (Horiba LabRAM HR Evolution, Japan).

2.6. Electrochemical performance testing

The electrochemical properties of electrode materials and devices were characterized using the Autolab PGSTATs electrochemical workstation in Switzerland. A three-electrode system was employed for testing in a 0.5M LiCl aqueous solution, with the working electrode being $LiFePO_4$, the counter electrode being platinum, and the reference electrode being K/KCl. The characterization included cyclic voltammetry (CV) with a test voltage window of −0.99 to 0.99 V and a scanning rate of 0.2 mV/s, as well as multiple tests and electrochemical impedance spectroscopy (EIS) with a scanning frequency range of 0.001 Hz–100 kHz.

2.7. Lithium extraction

The R-$LiFePO_4$ electrode was used as the anode, $FePO_4$ prepared from S-$LiFePO_4$ was used as the cathode, saturated KCl was used as the reference electrode, and IONAC MA-3475 was used as the anion-selective membrane, and 0.1 M LiCl and simulated brine were added to the cathode compartment, while 0.1 M NaCl and KCl were added to the anode compartment and 0.8 and 0.3 V were applied, respectively. At the end of each cycle, 1 mL of solution was taken in the anode chamber for dilution, and the amount of Li^+ removed from the solution was analyzed by inductively coupled plasma optical emission spectrometer (ICP, Thermo Fisher, USA). Afterward, the positions of the cathode and anode electrodes were reversed, and the electrolysis continued for the next cycle.

2.8. Study of the effect of impurity ions on Li^+ selectivity in real brines

The West Taijinar old brine was used as the research subject. The West Taijinar old brine (1:1) was added to the anode chamber and KCl was added to the cathode chamber. The anode consisted of R-$LiFePO_4$ electrode, while $LiFePO_4$ was used as the cathode. A voltage of 0.3 V was applied, and the concentrations of Li^+, Na^+, Mg^{2+} and K^+ were analyzed using ICP.

3. Results and discussion

3.1. Structure and morphology characterization of materials

Fig. S1 shows the oxidation of S-$LiFePO_4$ in $Na_2S_2O_4$ solution. The figure demonstrates that the oxidation rate is rapid, with the lithium removal process completed within 10 min. The lithium deficiency of S-$LiFePO_4$ (Table S1) accelerates the delithiation reaction with the oxidizer. Compared to previous research on the electrolysis of commercial $LiFePO_4$ to prepare $FePO_4$, our method is approximately six times faster [22], demonstrating that the efficiency of FePO4 preparation can be significantly enhanced by using waste materials. Additionally, the crystal structure characteristics of S-$LiFePO_4$, R-$LiFePO_4$, and $FePO_4$ were further analyzed via X-ray diffraction (XRD). As shown in Fig. 2a, through the *Pnma* space group index JCPDS No.81-1173 $LiFePO_4$, it was observed that the diffraction peaks of S-$LiFePO_4$ and R-$LiFePO_4$ were essentially identical, indicating that the olivine-like structure of $LiFePO_4$ exhibited good structural stability and crystal structure [23]. Also, as Li was removed, the characteristic peaks on the (200), (210), and (020) crystal faces shifted to the right, and the corresponding *Pnma* space group (JCPDS No.34-0134$FePO_4$) appeared obvious $FePO_4$ characteristic peaks, with no other impurity peaks were found. This indicates that Li^+ was removed from $LiFePO_4$, yielding $FePO_4$. To verify this result, the XRD patterns of S-$LiFePO_4$ and $FePO_4$ were subjected to Rietveld refinement, as depicted in Fig. 2b–c, and the lattice parameters are given in Table S2. Compared with S-$LiFePO_4$, the lattice of $FePO_4$ contracted along [100] and [010], and slightly elongated along [001], which was consistent with the conclusions reported in the literature [24], further indicating that the sample obtained by oxidation was $FePO_4$.

The surface morphologies of S-$LiFePO_4$, R-$LiFePO_4$, and $FePO_4$ were analyzed using scanning electron microscopy (SEM). Fig. 2d–f illustrates irregular small particles for S-$LiFePO_4$ and R-$LiFePO_4$ with a particle size from approximately 0.2 to 1 μm. This suggests that the particles of S-$LiFePO_4$ remained intact after multiple cycles, and the calcination did not alter its morphology. Similarly, the structure of $FePO_4$ remained unchanged and largely consistent with R-$LiFePO_4$, indicating that the use of oxidants did not affect the fundamental morphology of the material. Additionally, transmission electron microscopy (TEM) was employed to further investigate the microstructure of S-$LiFePO_4$, R-$LiFePO_4$, and $FePO_4$. The magnified image in Fig. 2g and the Fast Fourier Transform (FFT) image in Fig. 2h–i revealed a carbon-coated surface of S-$LiFePO_4$ with gradually appearing disordered areas indicating structural degradation. The lattice spacing of 0.42 nm in the upper right area corresponded to the (101) crystal plane of olivine-type $LiFePO_4$. The Energy-dispersive X-ray spectroscopy (EDS) element mapping confirmed the even distribution of C, O, P, and Fe elements in the S-$LiFePO_4$ powder (Fig. S2). In contrast, R-$LiFePO_4$, exhibited no unnecessary areas post-sintering, with a lattice spacing of 0.43 nm corresponding to the (210) lattice surface of olivine-type $LiFePO_4$, indicative of good crystallinity (Fig. 2j). This suggests that sintering enhances the regularity of S-$LiFePO_4$ structure. Moreover, TEM enlargement in Fig. 2k demonstrated the regular microstructure of $FePO_4$ with high crystallinity, where the measured crystal plane spacing is 0.34 nm, corresponding to the (210) crystal plane of $FePO_4$ further confirming the successful preparation of $FePO_4$.

To verify the results above, X-ray photoelectron spectroscopy (XPS) was employed to analyze elemental compositions and valence states of S-$LiFePO_4$, R-$LiFePO_4$, and $FePO_4$, to further verify the success of the oxidation of S-$LiFePO_4$. The mechanism diagram of the oxidation of S-$LiFePO_4$ by $Na_2S_2O_8$ is shown in Fig. 3a. Under room temperature conditions, the oxidation rate of the oxidant sodium persulfate is relatively low. Therefore, thermal activation is employed. When the temperature is elevated to above 30 °C, the peroxy bond in $Na_2S_2O_8$ undergoes cleavage, generating highly oxidizing persulfate radical anions ($SO_4\cdot^-$). The possesses a lone pair of electrons, exhibits strong electron-accepting ability, and has a high oxidation capacity [25](The comparison of the oxidizing properties of persulfates can be found in the supporting information). It is capable of oxidizing Fe^{2+} in S-$LiFePO_4$ to Fe^{3+}.The olivine structure of $LiFePO_4$ will not be changed while lithium is removed, resulting in $FePO_4$ in the under-lithium state. The reaction equation is shown in equations 2-1 and 2-2.

$$S_2O_8^{2-} \rightarrow 2SO_4\cdot^- \quad (3\text{-}1)$$

$$SO4\cdot^- + S\text{-}\ LiFePO_4 \rightarrow FePO_4 + Li^+ + SO_4^{2-} \quad (3\text{-}2)$$

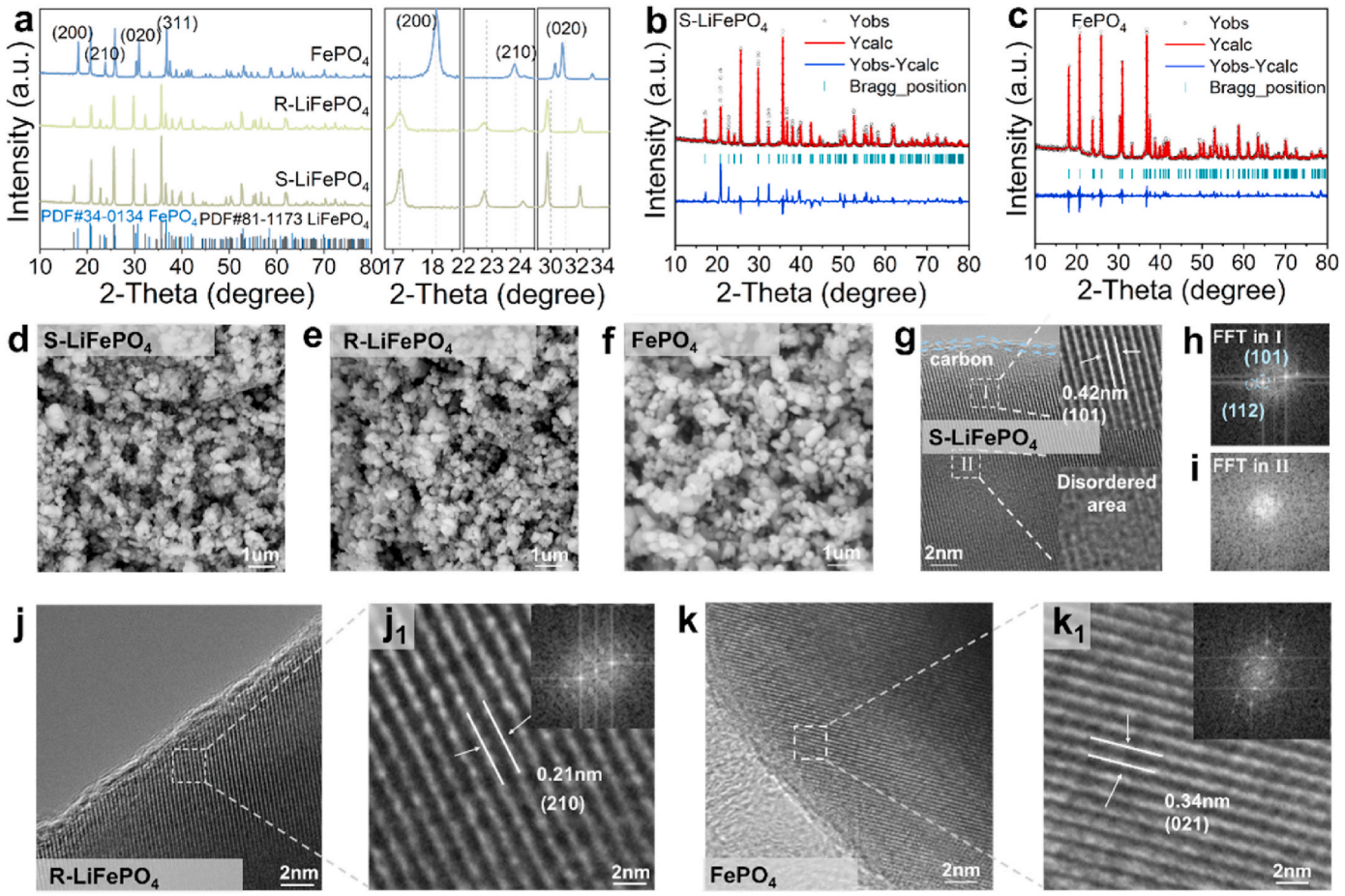

Fig. 2. Phase analysis and morphological characterization of samples. (a) XRD patterns; Refinement XRD comparison of (b) S-LiFePO$_4$, (c) FePO$_4$;SEM images of (d) S-LiFePO$_4$, (e) R-LiFePO$_4$, (f) FePO$_4$; TEM images of (g–i) S-LiFePO$_4$, (j and j$_1$) R -LiFePO$_4$, (k and k$_1$) FePO$_4$.

The full spectrum diagram (Fig. S3) revealed the presence of five elements: Li, Fe, P, O, and C in S-LiFePO$_4$. Notably, characteristic peak binding energies at 726.3 eV and 711.7 eV in Fe 2P spectrum correspond to the Fe^{3+} states of Fe $2p_{1/2}$ and Fe $2p_{3/2}$, respectively (Fig. 3b). Furthermore, elemental composition and relative content of S-LiFePO$_4$ were determined using inductively coupled plasma atomic emission spectroscopy (ICP-AES), revealing a lower relative content of Li (42.819 mg/g) compared to the theoretical value (44 mg/g), suggesting lithium loss in the S-LiFePO$_4$ material. Further evidence that the loss of lithium was associated with the formation of Fe^{3+} within the LiFePO$_4$ crystal structure [26]. Following calcination in an argon atmosphere, a significant increase in Fe^{2+} content accompanied by a decrease in Fe^{3+} content indicated effective repair of S-LiFePO$_4$ (Fig. 3c). In addition, oxidation with $Na_2S_2O_8$ led to a shift in the Fe $2P_{3/2}$ characteristic peak of S-LiFePO$_4$ from 709.51 eV to 711.81 eV, indicating oxidation of Fe^{2+} to Fe^{3+} (Fig. 3d). However, alongside Fe^{3+}, the presence of a small amount of Fe^{2+} in FePO$_4$, indicating that there is a small amount of LiFePO$_4$ existed due to the rapid oxidation reaction and incomplete delithiation, resulting in the presence of residual LiFePO$_4$. Through the determination of the lithium content, it is found that 98 % has been oxidized to FePO$_4$. Although a small amount of Li^+ exists, as shown in the XRD pattern of Fig. 2a, it does not affect the preparation of FePO$_4$. Most of the Fe^{2+} in LiFePO$_4$ was converted to Fe^{3+} in FePO$_4$, demonstrating the successful preparation of FePO$_4$. Additionally, the ratio of C-O-C to C-C peak area in the C 1s spectrum was found to be smaller in R-LiFePO$_4$ (0.15) compared to S-LiFePO$_4$ (0.18) (Fig. 3e). According to previous research, a smaller ratio of peak area indicates fewer defects in the carbon layer [27], suggesting that R-LiFePO$_4$ exhibited improved structural integrity and confirming the effectiveness of S-LiFePO$_4$ repair.

Raman spectroscopy further evaluated the degree of carbon graphitization in the samples (Fig. 3f). The I_D/I_G value of S-LiFePO$_4$ (1.036) exceeded that of R-LiFePO$_4$ (0.973) and FePO$_4$ (0.843), indicating a higher degree of defects in the original sample. Additionally, the degree of carbon graphitization increased in the repaired samples, providing additional evidence for the efficacy of S-LiFePO$_4$ repair. Moreover, infrared spectra analysis (Fig. 3g) revealed similar wavelengths of functional groups in S-LiFePO$_4$, R-LiFePO$_4$, and FePO$_4$, further supporting the stable olivine-like structure of LiFePO$_4$.

3.2. Characterization of electrochemical properties and the lithium intercalation and deintercalation performance of the R-LiFePO$_4$/FePO$_4$ system

To further investigate the lithium intercalation and deintercalation capabilities of S-LiFePO$_4$ and R-LiFePO$_4$, the electrochemical performance of S-LiFePO$_4$ and R-LiFePO$_4$ was evaluated. Fig. 4a illustrates the performance rate of the electrodes within the range of 0.1–3C. The discharge capacity of both materials decreased with an increasing rate. However, R-LiFePO$_4$ maintained a higher discharge capacity than S-LiFePO$_4$ at each rate. Even at a high rate of 3C, R-LiFePO$_4$ performed a significantly higher discharge specific capacity (75.5 mAh/g) compared to S-LiFePO$_4$ (46 mAh/g). Additionally, when the rate is reduced back to 0.1C, the R-LiFePO$_4$ electrode showed a substantial recovery of its initial capacity (120.5 mAh/g), indicating superior reversibility [28]. Furthermore, as illustrated by the EIS and the high frequency region of the two electrodes, S-LiFePO$_4$ exhibits a greater charge transfer resistance than R-LiFePO4, at 6.26Ω and16.8Ω, respectively (Fig. 4b). In addition, the ion transport resistance of S-LiFePO$_4$ is higher during ion

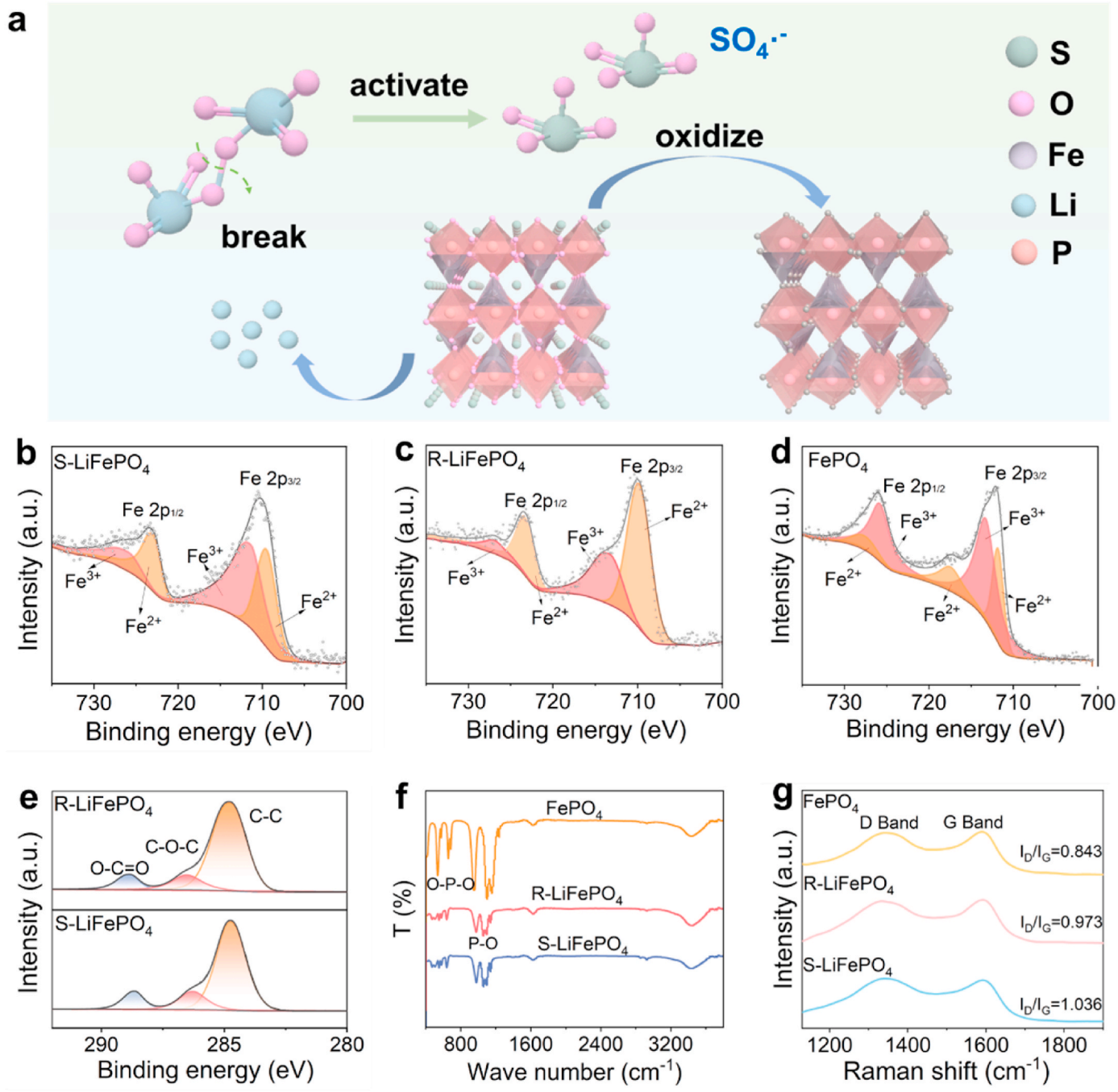

Fig. 3. XPS and Infrared spectra of the samples. (a) Mechanism diagram of $FePO_4$ preparation by oxidation reaction; high-resolution spectra of (b–d) Fe 2p and (e) C 1s; (f) Raman spectra of the samples; (g) Infrared spectra of the samples.

transport. This indicates that the repair of S-$LiFePO_4$ not only enhances the electron transport capacity of the material, but also increases the transmission rate of Li^+ into the electrode in the electrolyte [29].

The charge/discharge curves of the S-$LiFePO_4$ and R-$LiFePO_4$ were also tested (Fig. 4c), a relatively stable voltage plateau appeared around 0.15 V. Moreover, the R-$LiFePO_4$ (51 mV) exhibited lower polarization and larger charge/discharge capacity compared with the S-$LiFePO_4$ (78 mV), which further indicated that Li^+ in the R-$LiFePO_4$ migrated faster and had a good electrochemical power performance. In addition, the long cycle performance of $LiFePO_4/FePO_4$ in 0.1 M LiCl was further measured (Fig. 4d), After 40 cycles, the initial discharge capacity of S-$LiFePO_4$ (85.1 mAh/g) was much lower than that of R-$LiFePO_4$ (143 mAh/g), and the capacity retention rate of S-$LiFePO_4$ (84.6 %) was reduced compared to that of R-$LiFePO_4$ (86.9 %), indicating that the repair of $LiFePO_4$ increased the cycle stability of the electrode.

Based on the electrochemical performance, the feasibility and lithium extraction capability of the R-$LiFePO_4/FePO_4$ system in electrochemical delithiation method for lithium extraction from salt lakes. Firstly, the lithium extraction performance in 0.1 M LiCl was investigated. As shown in Fig. 4e and f, after 5 cycles, the capacity of each lithium release did not change much, and the average lithium capacity (34.32 mg/g) and lithium efficiency (77.99 %) were much higher than the average lithium capacity (23.25 mg/g) and lithium efficiency (52.84 %) of S-$LiFePO_4$. This means that the R-$LiFePO_4/FePO_4$ system had good lithium extraction performance. After high-temperature calcination, its structure was more regular and the deintercalation ability of Li^+ was

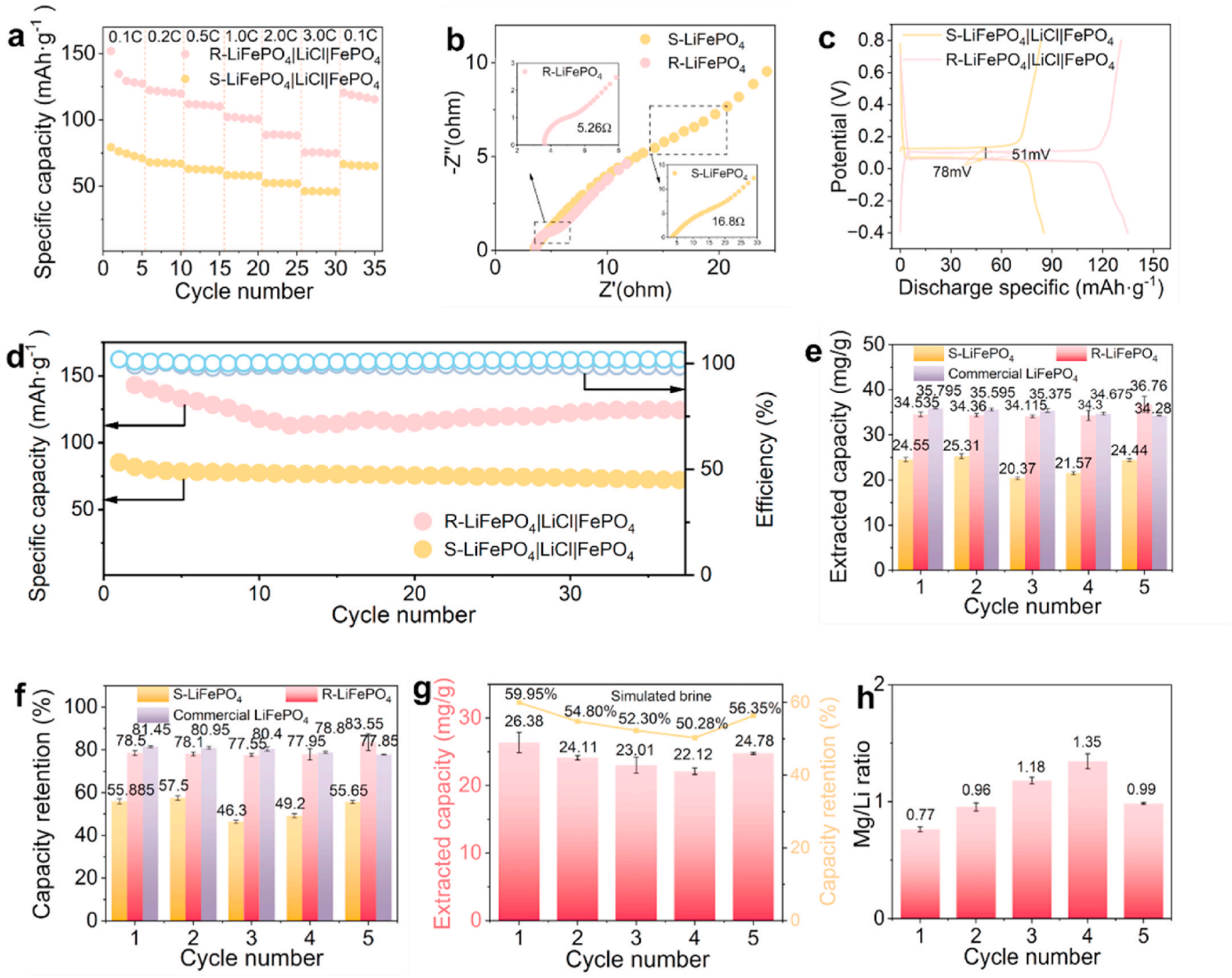

Fig. 4. Electrochemical tests of S-LiFePO$_4$ and R-LiFePO$_4$ electrode. (a) Discharge capacity of S-LiFePO$_4$ and R-LiFePO$_4$ at different rates in 0.1 M LiCl; (b) EIS in 0.5 M LiCl; (c) The charge/discharge curves of S-LiFePO$_4$ and R-LiFePO$_4$ in 0.1 M LiCl; (d) Long-cycle performance of S-LiFePO$_4$ and R-LiFePO$_4$ in 0.1 M LiCl. The Extraction of lithium properties at LiFePO$_4$/FePO$_4$ electrode. (e) Li^+ de-intercalation capacity of S-LiFePO$_4$ and R-LiFePO$_4$ as the anode in 0.1 M LiCl; (f) detachment efficiency; (g) repair the circulating Li^+ de-intercalation capacity of R-LiFePO$_4$/FePO$_4$ system and lithium extraction efficiency; (h) Mg/Li of R-LiFePO$_4$/FePO$_4$ system in 0.1 M LiCl.

improved. In addition, compared with the lithium extraction performance of commercial LiFePO$_4$ in pure lithium solution, the two methods had similar lithium extraction efficiency, and the new method was simple to operate and more cost-saving [15]. Furthermore, the viability of utilizing waste battery materials for lithium extraction through electrochemical de-intercalation method has been demonstrated.

Moreover, the lithium extraction efficiency of the system in the brine was studied with the artificial brine, and the concentration of each ion in the brine was simulated (Table S3) [30]. The lithium extraction performance is shown in Fig. 4g the average lithium removal capacity of the anode is 24.08 mg/g, and the lithium removal efficiency is 54.73 %. The first lithium removal capacity is 26.38 mg/g, which is higher compared with the other several times because part of the first lithium removal capacity is Li^+ from the LiFePO$_4$ electrode itself. Fig. 4h shows that Mg/Li decreased from 37 to 0.77, indicating that the R-LiFePO$_4$/FePO$_4$ system has good applicability in brine with a high magnesium-lithium ratio.

3.3. Study on the selectivity of R-LiFePO$_4$/FePO$_4$ system to impurity ion in brine

Most of Chinese salt lakes have a high viscosity, a high Mg/Li ratio, and a low lithium concentration. In addition, the brine composition is complicated by the presence of a large number of impurity ions, such as Na^+, K^+, and Mg^{2+} will have a certain effect on the extraction of Li^+. Therefore, it is crucial to study the separation effect of this system on Li^+ and different impurity ions. Firstly, the electrochemical behavior of the prepared FePO$_4$ electrode was studied in various solutions with a certain concentration of 0.5 M, including LiCl, NaCl, KCl, and MgCl$_2$ (Fig. 5a–d). When the cations are intercalated in the process of FePO$_4$, the intercalation potentials and the degree of difficulty of each type of cation are different. The order of their intercalation potential is: Li^+ (0.04 V) < Na^+ (−0.23 V) < Mg^{2+} (−0.61 V) < K^+ (−0.74 V). Since the more positive the intercalation potential, the easier it is to intercalate, indicating that Li^+ is the easiest to intercalate in FePO$_4$, and K^+ is the most difficult to intercalate [31]. Besides, in the process of cation removal, there are no obvious oxidation peaks for other cations except for Li^+ and Na^+. This indicates that due to the electronegativity or larger ionic radius of K^+

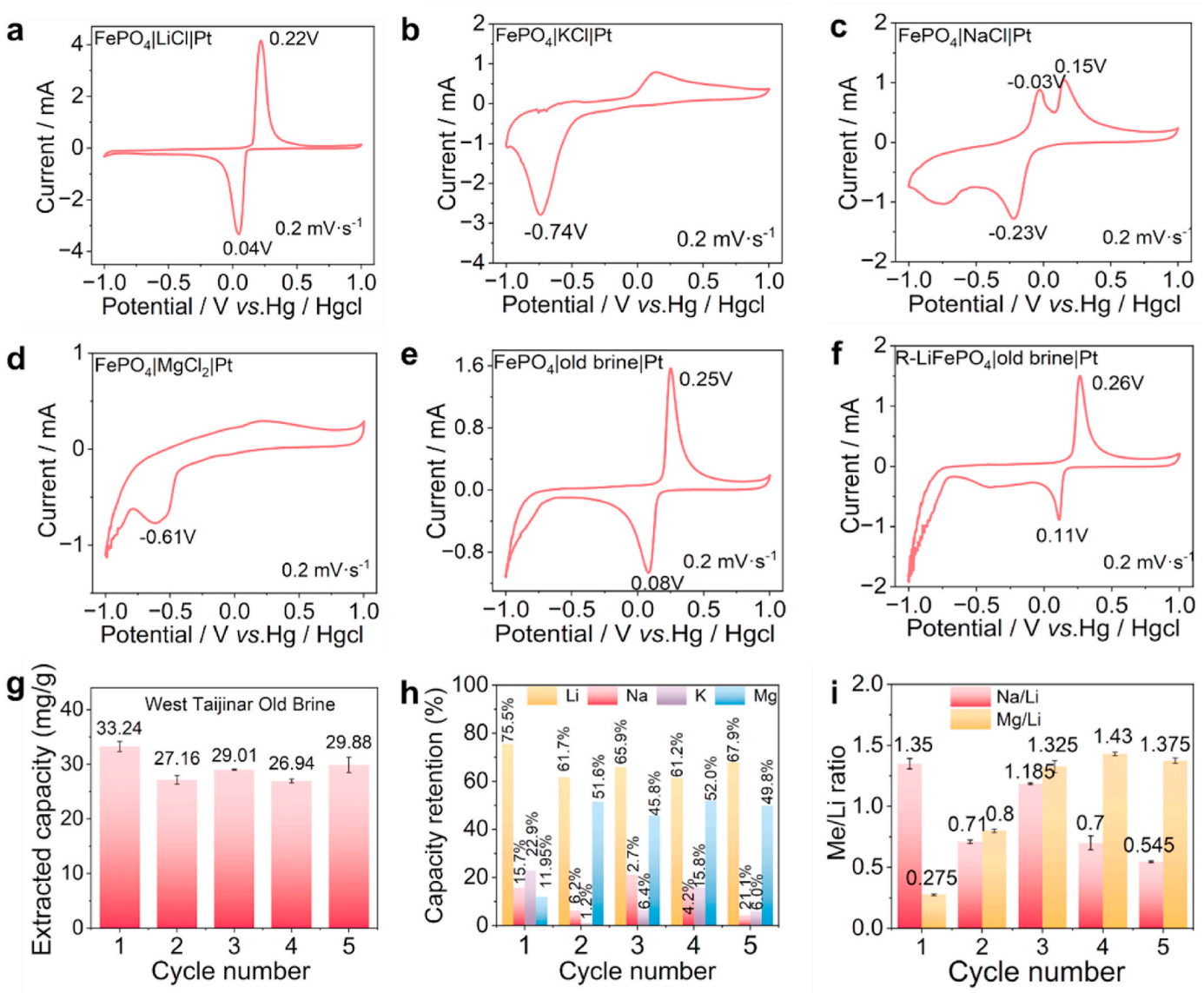

Fig. 5. Circular voltametric test curve of the $FePO_4$ electrode prepared by oxidation method at 0.2 mV/s (a) 0.5 mol/L LiCl, (b) 0.5 mol/L KCl, (c) 0.5 mol/L NaCl; (d) 0.5 mol/L $MgCl_2$; (e) old halogen; (f) cyclic voltammetric test curve of R-$LiFePO_4$ electrode in old brine; (g) circulating lithium extraction capacity of R-$LiFePO_4$/$FePO_4$ system in old brine; (h) removal efficiency of R-$LiFePO_4$/$FePO_4$ system in Li, Na, K and Mg in old brine; (i) Na/Li ratio to Li ratio of Mg/Li ratio in old brine.

and Mg^{2+}, they are embedded in $FePO_4$ at a negative voltage, which makes them lose their electrochemical activity, hindering the removal of K^+ and Mg^{2+}. To further demonstrate the selectivity of this electrode system towards Li^+, the electrochemical behaviors of R-$LiFePO_4$ in solutions containing different impurity ions are presented in Fig. S4. It can be observed that the intercalation potentials are substantially consistent. This indicates that both R-$LiFePO_4$ and $FePO_4$ exhibit superior selectivity for Li^+. Therefore, the potential can be controlled to achieve the de-intercalation of lithium ions by the ease of intercalation and dislodging of each cation.

Furthermore, the cation de-intercalation behavior in West Taijinar old brine was investigated, and the concentration of each cation in West Taijinar old brine was shown in Table S4 [32]. The cyclic voltammetry tests were first carried out on iron phosphate and lithium iron phosphate (Fig. 5e–f). Although the ionic environments in the old brine were very complicated, there was only one oxidation peak and reduction peak in the prepared $FePO_4$ and R-$LiFePO_4$ electrodes, respectively, and the oxidation-reduction potentials were 0.25 V and 0.08 V; 0.26 V and 0.11 V, which are consistent with the dislodging and intercalation potentials of Li^+. This indicates that the electrode material has an efficient Li^+ selectivity in the old brine. The de-intercalation potential was optimized at 0.3 V and conducted electrochemical de-intercalation method experiments in old halogen by observing the electrochemical behaviors. Relative results are shown in Fig. 5g–i. Fig. 5g shows the lithium extraction capacity of this system in the old brine after five cycles. It shows that the capacity of five cycles is relatively stable, and the average capacity can reach 29.25 mg/g. Fig. 5h shows the efficiency of the four ions in old brine to be de-intercalated in this system, and the de-intercalation of K^+ in this system is less, and it doesn't have much effect on this system. However, a certain amount of Na^+ still undergoes de-intercalation in this system. When the concentrations of Na^+ and Li^+ are of the same order of magnitude, due to the difference in the ionic radii between Na^+ and Li^+ and based on the electrochemical behaviors of their intercalation into the $LiFePO_4$ electrode, there also exists a discrepancy in their intercalation potentials. As a result, the $LiFePO_4$ electrode exhibits favorable selectivity towards Li^+. Nevertheless, in brine, the concentration of Na^+ is considerably high while that of Li^+ is extremely low. During the intercalation process into the $LiFePO_4$ electrode, a fraction of Na^+ will, under the influence of kinetic forces, intercalate into the material, which exerts a certain impact on the

selectivity of the electrode for Li^+ [12].The efficiency of Li^+ removal is higher than all other cations, which indicates that the system has a high selectivity for lithium ions. Although the removal efficiency of Mg^{2+} is higher than that of other impurity ions, the magnesium-lithium ratio decreased from 61.7 to 0.8 and the sodium-lithium ratio decreased from 3.42 to 0.545 in five cycles of the system (Fig. 5i). The above study shows that electrochemical de-intercalation of lithium in this system not only has good lithium extraction efficiency but also has good lithium-ion selectivity.

The above work has proved the feasibility of using waste electrode material in the positive electrode and $FePO_4$ material prepared by oxidation in the negative electrode to extract lithium by electrochemical stripping method. Not only that, the use of S-$LiFePO_4$ also has great advantages in terms of cost and efficiency in preparing $FePO_4$. In terms of cost, the use of S-$LiFePO_4$ is about 56 % less than commercial $LiFePO_4$, and in terms of efficiency, the use of S-$LiFePO_4$ chemical oxidation process to prepare $FePO_4$ is 24 times faster than traditional methods. This gives S-$LiFePO_4$ a great advantage in the extraction of lithium from salt lakes. (Please refer to supporting information for specific data).

4. Conclusions

In summary, this study proposed a new electrochemical strategy for lithium extraction from salt lake brine using the $LiFePO_4$/$FePO_4$ system based on the materials from spent lithium-ion batteries. Compared to the traditional $LiFePO_4$ systems, this system not only has excellent delithiation capacity, efficiency, and lithium-ion selectivity, but also offers lower preparation costs. It takes only about 10 min to delithium from $LiFePO_4$ to $FePO_4$, and this system has a lithium extraction capacity of 34.32 mg/g in pure lithium solution, with a delithiation efficiency of 77.99 %. In addition, it has a delithiation capacity of 29.25 mg/g for actual brine, with an efficiency of 66.5 %. The Mg/Li ratio decreased from 61.4 to 0.8. Considering cost, efficiency, and selectivity, the use of S-$LiFePO_4$ for lithium extraction from brine is promising for large-scale industrial applications. This study not only provides a new approach for lithium extraction from brine, but also develops an effective strategy for recycling spent lithium-ion batteries.

CRediT authorship contribution statement

Yawen Gao: Writing – original draft, Methodology, Data curation, Conceptualization. **Luxiang Ma:** Writing – review & editing, Investigation, Funding acquisition, Formal analysis, Conceptualization. **Shuaifei Zhao:** Writing – review & editing, Formal analysis. **Chunxi Hai:** Funding acquisition, Formal analysis. **Tiandong Chen:** Writing – review & editing, Formal analysis. **Junyi Zhang:** Formal analysis, Conceptualization. **Yan Zhao:** Writing – review & editing, Formal analysis. **Yanxia Sun:** Writing – review & editing, Formal analysis. **Shengde Dong:** Writing – review & editing, Formal analysis. **Xin He:** Writing – review & editing, Formal analysis. **Qi Xu:** Writing – review & editing, Formal analysis. **Xiaowang Wu:** Writing – review & editing, Formal analysis, Conceptualization. **Caixiong Quan:** Writing – review & editing, Formal analysis. **Hongli Su:** Writing – review & editing, Formal analysis, Conceptualization. **Yuan Zhou:** Writing – review & editing, Funding acquisition, Conceptualization.

Declaration of competing interest

The authors declare that we do not have any commercial or associative interest that represents a conflict of interest in connection with the work submitted entitled *"Cost-Effective and Efficient Preparation of $FePO_4$ Electrodes from Spent $LiFePO_4$ Batteries for Enhanced Lithium Extraction from Salt Lakes"*.

Acknowledge

This research received funding from the Haixi Science and Technology planning Project, under Grant No. 2024-JC-Q01.

Appendix A. Supplementary data

Supplementary data to this article can be found online at https://doi.org/10.1016/j.mtener.2025.101848.

Data availability

Data will be made available on request.

References

[1] M.A. Hannan, M.S.H. Lipu, A. Hussain, A. Mohamed, A review of lithium-ion battery state of charge estimation and management system in electric vehicle applications: challenges and recommendations, Renew. Sustain. Energy Rev. 78 (2017) 834–854, https://doi.org/10.1016/j.rser.2017.05.001.
[2] Z. Gao, M. Huang, L. Yang, Y. Feng, Y. Ding, P. Shao, X. Luo, Review of preferentially selective lithium extraction from spent lithium batteries: principle and performance, J. Energy Chem. 78 (2023) 253–261, https://doi.org/10.1016/j.jechem.2022.11.061.
[3] X. Zhao, S. Yang, Y. Hou, H. Gao, Y. Wang, D.A. Gribble, V.G. Pol, Recent progress on key materials and technical approaches for electrochemical lithium extraction processes, Desalination 546 (2023) 116189, https://doi.org/10.1016/j.desal.2022.116189.
[4] V. Flexer, C.F. Baspineiro, C.I. Galli, Lithium recovery from brines: a vital raw material for green energies with a potential environmental impact in its mining and processing, Sci. Total Environ. 639 (2018) 1188–1204, https://doi.org/10.1016/j.scitotenv.2018.05.223.
[5] Y. Sun, Q. Wang, Y. Wang, R. Yun, X. Xiang, Recent advances in magnesium/lithium separation and lithium extraction technologies from salt lake brine, Separation and Purification Technology 256 (2021) 117807, https://doi.org/10.1016/j.seppur.2020.117807.
[6] B. Swain, Recovery and recycling of lithium: a review, Separation and Purification Technology 172 (2017) 388–403, https://doi.org/10.1016/j.seppur.2016.08.031.
[7] W. Xu, L. He, Z. Zhao, Lithium extraction from high Mg/Li brine via electrochemical intercalation/de-intercalation system using LiMn2O4 materials, Desalination 503 (2021) 114935, https://doi.org/10.1016/j.desal.2021.114935.
[8] Z. Zhao, G. Liu, H. Jia, L. He, Sandwiched liquid-membrane electrodialysis: lithium selective recovery from salt lake brines with high Mg/Li ratio, J. Membr. Sci. 596 (2020) 117685, https://doi.org/10.1016/j.memsci.2019.117685.
[9] W. Xu, D. Liu, X. Liu, D. Wang, L. He, Z. Zhao, Highly selective and efficient lithium extraction from brines by constructing a novel multiple-crack-porous LiFePO4/FePO4 electrode, Desalination 546 (2023) 116188, https://doi.org/10.1016/j.desal.2022.116188.
[10] D. Liu, W. Xu, J. Xiong, L. He, Z. Zhao, Electrochemical system with LiMn2O4 porous electrode for lithium recovery and its kinetics, Separation and Purification Technology 270 (2021) 118809, https://doi.org/10.1016/j.seppur.2021.118809.
[11] X. Meng, Y. Jing, J. Li, Z. Sun, Z. Wu, Electrochemical recovery of lithium from brine by highly stable truncated octahedral LiNi0.05Mn1.95O4, Chem. Eng. Sci. 283 (2024) 119400, https://doi.org/10.1016/j.ces.2023.119400.
[12] C. Liu, Y. Li, D. Lin, P.-C. Hsu, B. Liu, G. Yan, T. Wu, Y. Cui, S. Chu, Lithium extraction from seawater through pulsed electrochemical intercalation, Joule 4 (2020) 1459–1469, https://doi.org/10.1016/j.joule.2020.05.017.
[13] S. Sun, X. Yu, M. Li, J. Duo, Y. Guo, T. Deng, Green recovery of lithium from geothermal water based on a novel lithium iron phosphate electrochemical technique, J. Clean. Prod. 247 (2020) 119178, https://doi.org/10.1016/j.jclepro.2019.119178.
[14] R.-x. Yin, W.-g. Zhu, Z.-w. Zhao, w.-h. Xu, X.-h. Liu, L.-h. He, Lithium recovery from brine by PEG-modified porous LiFePO4/FePO4 electrode system, Separation and Purification Technology 338 (2024) 126375, https://doi.org/10.1016/j.seppur.2024.126375.
[15] L. He, W. Xu, Y. Song, Y. Luo, X. Liu, Z. Zhao, New insights into the application of lithium-ion battery materials: selective extraction of lithium from brines via a rocking-chair lithium-ion battery system, Global Challenges 2 (2018) 1700079, https://doi.org/10.1002/gch2.201700079.
[16] C. Crouzet, N. Recham, F. Brunet, N. Findling, R. David, M.-T. Sougrati, A novel route for FePO4 olivine synthesis from sarcopside oxidation, Solid State Sci. 62 (2016) 29–33, https://doi.org/10.1016/j.solidstatesciences.2016.10.013.
[17] J. Xiong, L. He, D. Liu, W. Xu, Z. Zhao, Olivine-FePO4 preparation for lithium extraction from brines via Electrochemical De-intercalation/Intercalation method, Desalination 520 (2021) 115326, https://doi.org/10.1016/j.desal.2021.115326.
[18] X. Qiu, C. Wang, L. Xie, L. Zhu, X. Cao, X. Ji, Challenges and perspectives towards direct regeneration of spent LiFePO4 cathode, J. Power Sources 602 (2024) 234365, https://doi.org/10.1016/j.jpowsour.2024.234365.
[19] M. Klett, R. Eriksson, J. Groot, P. Svens, K. Ciosek Högström, R.W. Lindström, H. Berg, T. Gustafson, G. Lindbergh, K. Edström, Non-uniform aging of cycled commercial LiFePO4//graphite cylindrical cells revealed by post-mortem analysis,

J. Power Sources 257 (2014) 126–137, https://doi.org/10.1016/j.jpowsour.2014.01.105.
[20] J. Vetter, P. Novák, M.R. Wagner, C. Veit, K.C. Möller, J.O. Besenhard, M. Winter, M. Wohlfahrt-Mehrens, C. Vogler, A. Hammouche, Ageing mechanisms in lithium-ion batteries, J. Power Sources 147 (2005) 269–281, https://doi.org/10.1016/j.jpowsour.2005.01.006.
[21] M. Du, J.-Z. Guo, S.-H. Zheng, Y. Liu, J.-L. Yang, K.-Y. Zhang, Z.-Y. Gu, X.-T. Wang, X.-L. Wu, Direct reuse of LiFePO4 cathode materials from spent lithium-ion batteries: extracting Li from brine, Chin. Chem. Lett. 34 (2023) 107706, https://doi.org/10.1016/j.cclet.2022.07.049.
[22] J. Zhang, Y. Zhou, C. Hai, H. Su, Y. Zhao, Y. Sun, S. Dong, X. He, Q. Xu, T. Chen, J. Xiang, S. Huang, L. Ma, Enhancing lithium extraction efficiency from salt lake brines through three-dimensional conductive network-incorporated thick electrodes, Separation and Purification Technology 334 (2024) 126010, https://doi.org/10.1016/j.seppur.2023.126010.
[23] J. Zhang, Y. Zhou, C. Hai, Y. Gao, Y. Zhao, Y. Sun, S. Dong, X. He, Q. Xu, J. Chen, H. Su, L. Ma, Constructing the 3D-conductive network-incorporated thick electrodes via melamine foam for lithium extraction, Desalination 579 (2024) 117457, https://doi.org/10.1016/j.desal.2024.117457.
[24] G. Rousse, J. Rodriguez-Carvajal, S. Patoux, C. Masquelier, Magnetic structures of the triphylite LiFePO4 and of its delithiated form FePO4, Chem. Mater. 15 (2003) 4082–4090, https://doi.org/10.1021/cm0300462.
[25] Z. Liu, X. Ren, X. Duan, A.K. Sarmah, X. Zhao, Remediation of environmentally persistent organic pollutants (POPs) by persulfates oxidation system (PS): a review, Sci. Total Environ. 863 (2023) 160818, https://doi.org/10.1016/j.scitotenv.2022.160818.
[26] G. Ji, J. Wang, Z. Liang, K. Jia, J. Ma, Z. Zhuang, G. Zhou, H.-M. Cheng, Direct regeneration of degraded lithium-ion battery cathodes with a multifunctional organic lithium salt, Nat. Commun. 14 (2023) 584.
[27] M.C. Biesinger, B.P. Payne, A.P. Grosvenor, L.W.M. Lau, A.R. Gerson, R.S.C. Smart, Resolving surface chemical states in XPS analysis of first row transition metals, oxides and hydroxides: Cr, Mn, Fe, Co and Ni, Appl. Surf. Sci. 257 (2011) 2717–2730, https://doi.org/10.1016/j.apsusc.2010.10.051.
[28] J. Zhang, W. Su, B. Yi, Y. Guo, T. Deng, X. Yu, A new strategy for the preparation of highly stable and high-capacity electrodes for green electrochemical extraction of lithium, Chem. Eng. J. 454 (2023) 140416, https://doi.org/10.1016/j.cej.2022.140416.
[29] L. Xu, Y. Xiao, Z.-X. Yu, Y. Yang, C. Yan, J.-Q. Huang, Revisiting the electrochemical impedance spectroscopy of porous electrodes in Li-ion batteries by employing reference electrode, Angew. Chem. Int. Ed. 63 (2024) e202406054, https://doi.org/10.1002/anie.202406054.
[30] T. Ding, M. Zheng, S. Peng, Y. Lin, X. Zhang, M. Li, Lithium extraction from salt lakes with different hydrochemical types in the Tibet Plateau, Geosci. Front. 14 (2023) 101485, https://doi.org/10.1016/j.gsf.2022.101485.
[31] Z.-w. Zhao, X.-f. Si, X.-x. Liang, X.-h. Liu, L.-h. He, Electrochemical behavior of Li+, Mg2+, Na+ and K+ in LiFePO4/FePO4 structures, Trans. Nonferrous Metals Soc. China 23 (2013) 1157–1164, https://doi.org/10.1016/S1003-6326(13)62578-9.
[32] C. Zhu, Y. Dong, Z. Yun, Y. Hao, C. Wang, N. Dong, W. Li, Study of lithium exploitation from carbonate subtype and sulfate type salt-lakes of Tibet, Hydrometallurgy 149 (2014) 143–147, https://doi.org/10.1016/j.hydromet.2014.07.006.